Sources and Terminations of Callosal Axons Related to Binaural and Frequency Maps in Primary Auditory Cortex of the Cat

THOMAS J. IMIG AND JOHN F. BRUGGE
Department of Neurophysiology and Waisman Center on Mental Retardation and Human Development, University of Wisconsin Medical School, Madison, Wisconsin 53706

ABSTRACT The distributions of sources and terminals of callosal fibers in the high-frequency representation of AI were related to binaural and frequency maps in combined anatomical and electrophysiological experiments. Sources of callosal axons were retrogradely labeled with HRP. Distributions of axon terminals were determined by autoradiographic labeling with [^{3}H]-proline and anterograde degeneration following callosal section. Regions in which cells exhibit summation or ipsilateral dominance and suppression contain higher concentrations of sources and terminals of callosal fibers than do regions in which cells exhibit monaural contralateral responses or contralateral dominance and suppression. Callosal axon terminals aggregate into columns. In sections cut parallel to the cortical surface callosal columns take on complex forms that exhibit certain consistent features. Two prominent elongated columns separated by a narrow zone of sparse callosal innervation run in a rostrodorsal to caudoventral direction through AI crossing several octaves of the frequency representation. Ventral to these columns, along the AI-AII border, less densely labeled callosal columns are in evidence. Low frequency representations of AI are interconnected but details of their innervation patterns were not worked out. Outside of AI there are regions that contain complex configurations of callosal columns. Several morphologically distinct types of neurons, located in laminae III through VI, were retrogradely labeled following injections of HRP into the opposite AI. About 94% of callosal neurons are pyramidal cells of layers III and IV.

The sources and terminations of axons of the corpus callosum appear to be restricted in distribution to specific regions of the sensory representation in the primary visual and somatic sensory cortical areas of the cat and monkey. In area 17, the vertical meridian of the visual field is represented along the architectonic border between areas 17 and 18 and it is here that callosal axons arise and terminate. The remainder of area 17 in which more lateral portions of the visual field are represented neither contributes fibers to nor receives fibers from the callosal pathway (Berlucchi et al., '67; Choudhury et al., '65; Ebner and Myers, '65; Fisken et al., '75; Garey et al., '68; Hubel and Wiesel, '67; Wilson, '68). In primary somatic sensory cortex, the representations of the distal limbs appear devoid of callosal afferents whereas the representations of the face, trunk and tail receive callosal input (Ebner and Myers, '65; Jones et al., '75; Jones and Powell, '68, '69; Shanks et al., '75).

Considering the restricted distribution of the callosal fiber system in visual and somatic sensory cortices we wished to determine whether and to what extent a similar pattern of callosal innervation exists in the primary auditory field (AI) as well. Diamond et al. ('68) suggested that the low-frequency representation of AI may receive less dense callosal input than the high-frequency representation since the region dorsal to the upper tip of the posterior ectosylvian sulcus appears relatively free from callosal input. Pandya et al. ('69) have made a similar suggestion as a result of their experiments in the monkey. However, due to individual variation in the locations of the frequency maps with respect to cortical surface landmarks (Merzenich and Brugge, '73; Merzenich et al., '75) it is difficult to relate the pattern of callosal innervation derived in one experiment with frequency maps derived from others.

The purpose of this work is to relate in the same experiment the distribution of the sources and terminations of callosal axons to the sensory representation of AI. The cochleotopic organization of AI in the cat was initially worked out using the evoked potential technique (Woolsey and Walzl, '42) and recently has been studied in greater detail using microelectrode recording (Merzenich et al., '75). In addition to a frequency map, AI also contains a binaural representation in which cells with similar binaural properties form functional columns (Imig and Adrián, '77). In this paper we present evidence from combined anatomical and electrophysiological experiments that within AI the distributions of the sources and terminations of callosal axons are systematically related to both the frequency and binaural representations.

METHODS

Eighteen adult cats were used in these studies. All animals had clean external auditory canals and showed no signs of middle ear disease. Anesthesia was induced by intraperitoneal injection of sodium pentobarbital (40 mg/kg) and maintained with supplemental doses (10 mg/kg). Acute surgical procedures have been described previously (Imig and Adrián, '77). In eight cats, tritiated ([^{3}H]) proline (L-[5-^{3}H]-proline, specific activity 14-37 Ci/mmole, Amersham/Searle) was injected into AI. The solution contained 100 μCi of [^{3}H]-proline per microliter. In three cats, a 33-40% solution of horseradish peroxidase (HRP; Sigma type VI) dissolved in isotonic saline was injected into AI. Injections of [^{3}H]-proline or HRP were made using either a 1-μl Hamilton syringe or a calibrated glass micropipette with a tip diameter of 30-60 μm through which solutions were injected under pressure; the quantity injected is shown in figure legends. The corpus callosum was partially or completely sectioned in three other cats using sterile surgical procedures. Animals were allowed to survive six to eight days following surgery. The brains were then processed to stain degenerating axons and axon terminals using the technique of Fink and Heimer ('67).

Following injection of tracer compounds or section of the corpus callosum, electrophysiological recordings were made in each cat and the results later related to the anatomical maps. During recording sessions, the responses to tone pips of single neurons and clusters of neurons were studied. Animals were sacrificed immediately following the recording session. Details of the sound generating and recording systems have been described previously (Aitkin et al., '70; Imig and Adrián, '77).

Brains that received injections of [^{3}H]-proline were processed according to the technique described by Cowan et al. ('72). Tissue sections were cut at a thickness of 35-50 μm on a freezing microtome and exposed to Kodak NTB2 emulsion in the dark for three to four weeks.

Abbreviations

AES, anterior ectosylvian sulcus
AI, primary auditory field
AII, auditory field located ventral to AI between the anterior and posterior ectosylvian sulci
C, caudal
cc, corpus callosum
D, dorsal
fasc, fascicles
mgb, medial geniculate body
nr, no response
PES, posterior ectosylvian sulcus
R, rostral
SSS, suprasylvian sulcus
T, point at which the electrode initially touches the brain
V, ventral

Symbols used to describe neuron response properties

+, summation
B, no clearly defined best frequency
C−, contralateral dominance and suppression
−, contralateral dominance and suppression
I−, ipsilateral dominance and suppression
±, mixed summation and suppression
MC, monaural contralateral

Fig. 1 Route of the primary auditory callosal pathway.

A Nissl stained parasagittal section prepared for autoradiography. Six days prior to sacrifice, 20 μCi of [^{3}H]-proline was injected into each of 35 sites in AI. Arrows demark the limits of a dense accumulation of silver grains in the corpus callosum.

B,C Autoradiographs of coronal sections near the level of the posterior ectosylvian sulcus showing labeled fibers in the corpus callosum and its radiations. Seven days prior to sacrifice, AI in the left hemisphere received a single injection of 100 μCi of [^{3}H]-proline.

D Autoradiograph of a coronal section through AI in the right hemisphere with arrows pointing toward several callosal columns (same experiment as B and C). Dorsal is toward the right. Photomicrographs with black backgrounds in this figure (B, C and D) and in figures which follow were obtained using dark field illumination.

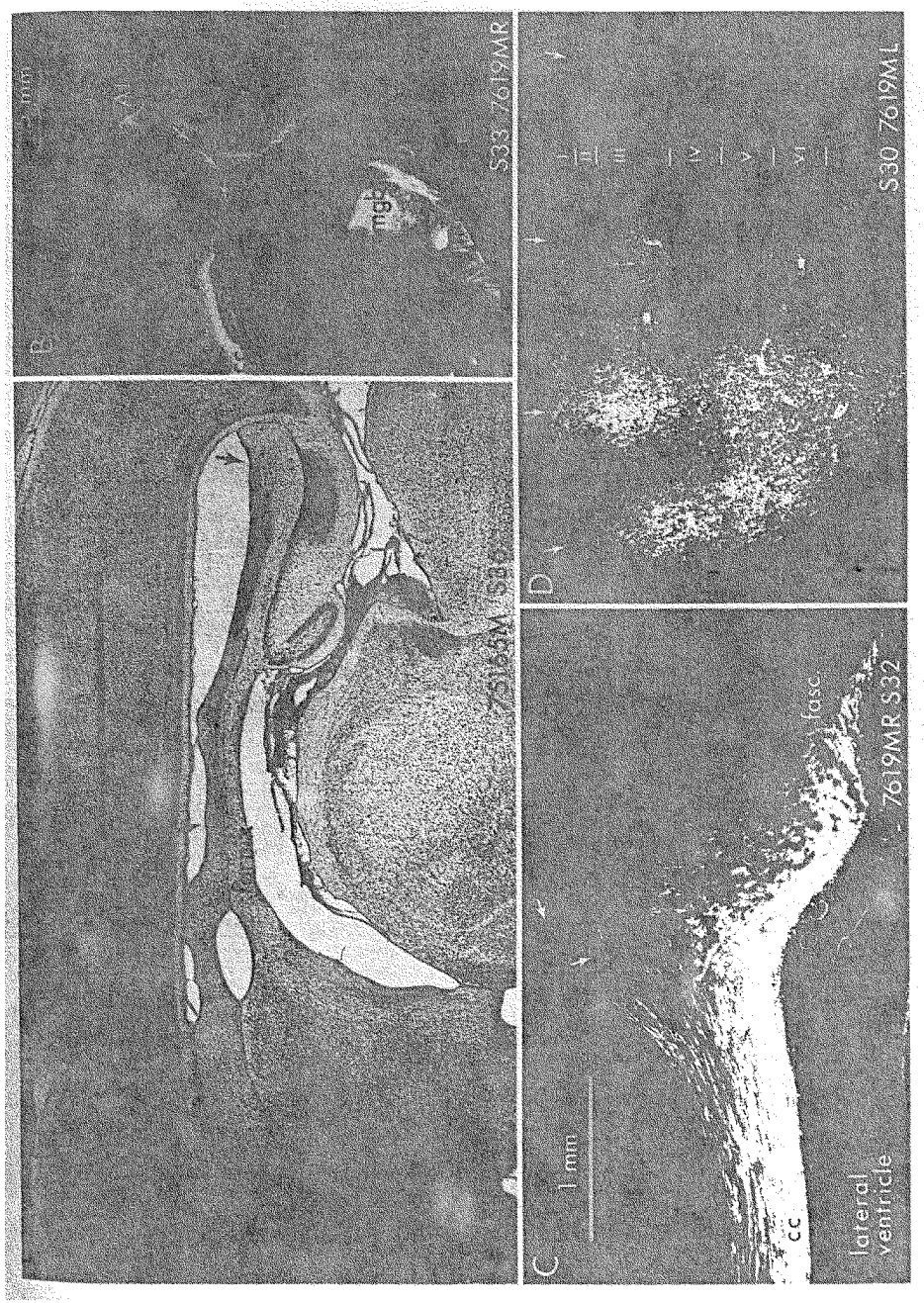

Figure 1

Brains that received injections of HRP were processed according to a protocol worked out by Caulwell and Merzenich (personal communication). Animals were perfused through the left ventricle with isotonic saline followed by two liters of a solution of 4% paraformaldehyde in 0.1 M phosphate buffer (pH 7.2); both solutions were at 4°C. After perfusion the brain was removed from the skull and stored overnight in a refrigerator in the buffered fixative. Over the next 24 hours while in the refrigerator, the brain was immersed in a 0.2 M phosphate buffer containing 5% sucrose followed by two changes of 0.2 M phosphate buffer containing 30% sucrose. Brains were cut frozen into sections 60 μm thick which were then placed into trizma buffer (pH 7.6, Sigma). To form the HRP reaction product, tissue sections were incubated for 30 minutes in a solution consisting of 100 mg of 3-3'diaminobenzidine tetrahydrochloride (Sigma) dissolved in 200 ml of trizma buffer to which two drops of 30% H_2O_2 had been added. Sections were then washed in three changes of trizma buffer and mounted on gelatinized slides.

The distribution of HRP labeled cells was related to binaural maps by plotting the positions of labeled cells on a drawing of a tissue section containing a reconstructed electrode track. In these experiments electrodes passed through the cortex nearly parallel to the cortical laminae. The positions of labeled cells found in segments of tissue sections containing the electrode track and in portions of the two tissue sections immediately adjacent to those segments were plotted either by use of an X-Y plotter coupled to the stage of a microscope or by marking the positions of labeled cells on photographs of tissue sections. The resulting drawing represented the positions of HRP labeled cells in a slab of cortex cut in the coronal plane. The slab was 180 μm in width (i.e., the thickness of 3 tissue sections) and included the reconstructed electrode track. The drawing was then divided into sectors by constructing lines parallel to radial cell columns that were spaced equally at the III-IV border (100 μm in one experiment, 200 μm in the other). Thus, each sector contained the positions and numbers of labeled HRP cells found in a radial column of cortical tissue through which passed an electrode track. The numbers and distributions of labeled cells within sectors were then related to the binaural responses of cells.

RESULTS

Route of the callosal pathway

Silver grains overlie the entire length of the AI callosal pathway in autoradiographs from experiments in which primary auditory cortex received an injection of [^{3}H]-proline seven to ten days prior to sacrifice (fig. 1B). Fibers leave the injection site and form a bundle which is flattened in the horizontal plane. Initially the bundle travels ventromedially around the fundus of the suprasylvian sulcus (arrows in fig. 1B) and then arcs dorsomedially to enter the callosal radiations above the lateral ventricle in a region located several millimeters caudal to the injection site. From this point fibers enter the corpus callosum. Upon leaving the callosal radiations in the hemisphere opposite the injection site, fibers course ventrolaterally around the fundus of the suprasylvian sulcus to reach their targets in AI. The locations of the other cortical and subcortical targets of the remaining fibers are beyond the scope of this report and will be described in a later paper.

The rostrocaudal extent of this pathway within the corpus callosum is best seen in parasagittal section. An autoradiograph from an experiment in which [^{3}H]-proline was injected at multiple sites in AI is illustrated in figure 1A. Arrows indicate the rostrocaudal extent of the distribution of silver grains in the corpus callosum. Silver grains are most densely aggregated in the caudal one-third of the corpus callosum except for the most caudal 1.5 mm which is free of label.

Throughout the pathway, silver grains cluster over fascicles of fibers (fig. 1C). Above the lateral aspect of the lateral ventricles in both hemispheres, fascicles break up to some extent as many fibers spread out dorsally and caudally (fig. 1B and 1C). After traveling for varying distances, these fibers bend (arrows in fig. 1C) and return to the main bundle.

Fig. 2 Laminar distribution of callosal afferents in AI.

A,B Autoradiograph of a tissue section through AI of the left hemisphere. Twenty-four hours prior to sacrifice, 100 μCi of [^{3}H]-proline was injected into each of seven sites in AI of the right hemisphere.

C,D Autoradiograph of a tissue section through the caudal bank of the posterior ectosylvian sulcus in the low frequency representation of AI in the left hemisphere. The lateral surface of the brain is toward the left. Twenty-five hours prior to sacrifice, 50 μCi of [^{3}H]-proline was injected at one location in the low frequency representation of AI in the right hemisphere.

Both tissue sections were cut in a plane extending rostrocaudally and nearly perpendicular to the lateral surface of AI.

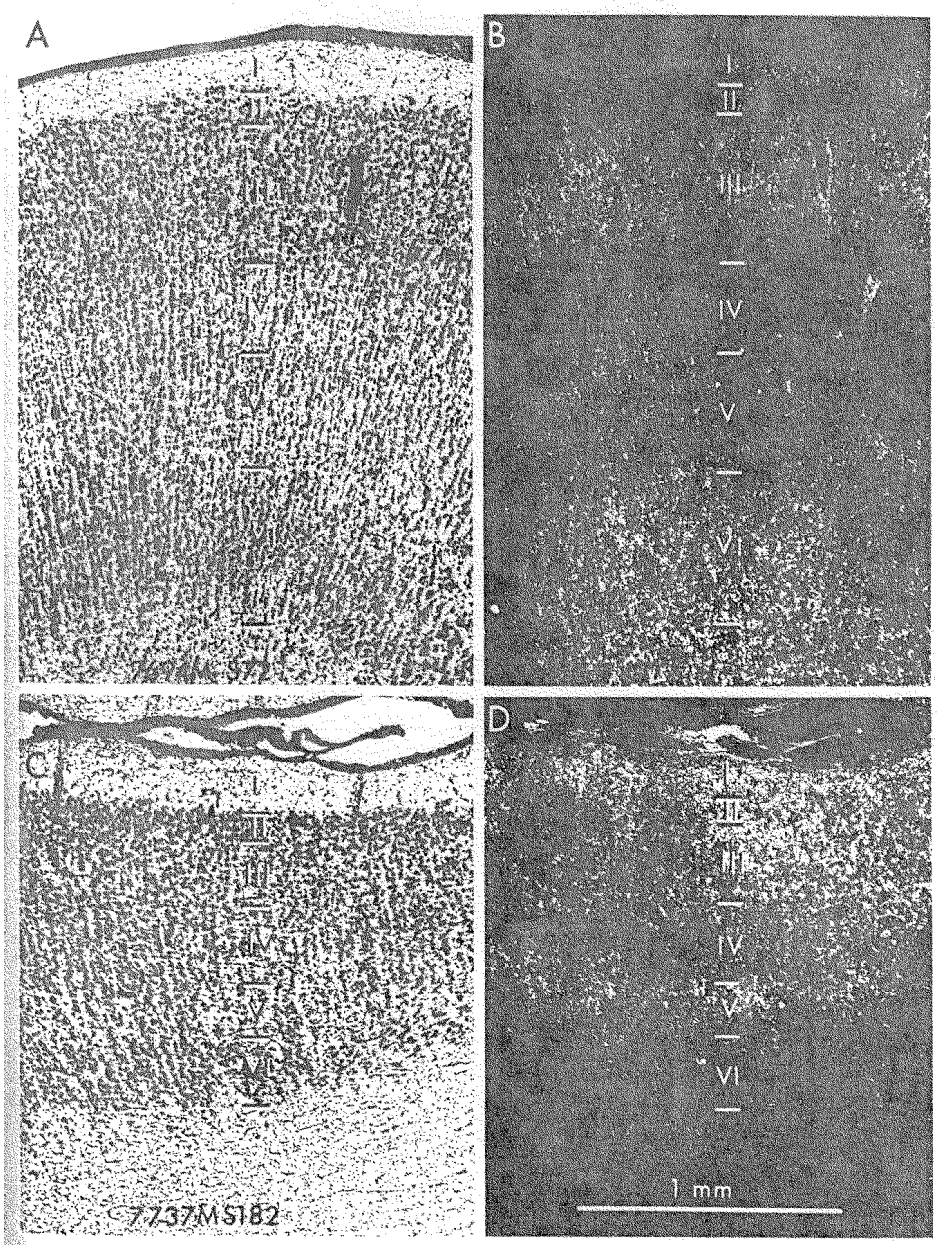

Figure 2

Callosal innervation pattern in primary auditory cortex

In autoradiographs from experiments in which the primary auditory field received a single injection of [^{3}H]-proline, silver grains aggregate within several distinct patches in AI of the hemisphere opposite the injection site. Arrows point to several of these patches in figure 1D. Generally the aggregates extend through all cortical layers. In areas between these dense aggregates, silver grains are present in lower concentrations. We refer to these dense aggregations as *callosal columns* using the terminology of Jones et al. ('75).

Silver grains generally accumulate more densely in certain laminae than others (fig. 2). As a rule, layer IV is less densely labeled than layer III. Layer I is as heavily or nearly as heavily labeled as layer III. Density of labeling of layer II in different brains varies considerably. A dense band of silver grains is found in the upper quarter of layer V in that part of AI which occupies the lateral surface of the brain (fig. 2B), but on the banks of the posterior ectosylvian sulcus this densely labeled band occupies well over half of the thickness of layer V (fig. 2D). An exceptional case in which silver grains appear uniformly distributed throughout layer V is seen in figure 1D. The density of labeling of layer VI varies among experiments. Layer VI was more lightly labeled than layer IV in brains receiving 50 μCi or less of [^{3}H]-proline (fig. 2D). On the other hand, layer VI was generally as heavily or more heavily labeled than layer III (fig. 2B) in brains receiving a total of 300-800 μCi. Figure 1D illustrates an intermediate pattern obtained in an experiment in which 100 μCi of [^{3}H]-proline was injected into AI of the opposite hemisphere. Here layer VI is less heavily labeled than layer III but more heavily labeled than layer IV. Both patterns were found in animals with survival times as short as 24 hours and as long as one week. It appears that the density of labeling of layer VI relative to the density of labeling of layers III and IV depends upon the quantity of [^{3}H]-proline which was injected.

Relationship between callosal columns and binaural columns

Most neurons within AI are sensitive to binaural stimulation. Neurons with similar binaural properties appear to form functional columns in the high-frequency representation of AI. In this section, we describe the relationship between binaural and callosal columns in AI.

During electrode penetrations into AI, the responses of single neurons were classified with respect to their monaural and binaural sensitivity at best frequency. The classification was based on the experimenters' judgments of the relative sizes of neural responses as viewed on the oscilloscope screen and has been described in a previous paper (Imig and Adrián, '77). Only a brief description is presented here. Initially monaural stimulation was presented to each ear. Often stimulation to one ear was capable of eliciting a larger response than stimulation to the other ear, a characteristic referred to as *aural dominance.* Binaural stimulation was then presented. Neurons whose responses to binaural stimulation were judged to be greater than their responses to stimulation of either ear alone were classified as showing *summation.* Neurons whose responses to binaural stimulation were smaller in size than their responses to monaural stimulation of the dominant ear were classified as showing *suppression.* For most neurons displaying suppression, the contralateral ear was dominant and hence are termed *contralateral dominant suppression* neurons. Some neurons were excited only by monaural stimulation to the contralateral ear and their binaural responses appeared identical to their monaural responses. Such neurons were classified as *monaural contralateral.*

It has been possible to relate the pattern of callosal columns to binaural columns by combining in the same experiment [^{3}H]-proline injections with microelectrode mapping of AI. Following a single injection of 10 μCi of [^{3}H]-proline into AI of the right hemisphere, binaural responses of neurons were studied during a tangential electrode penetration through AI of the left hemisphere. Figure 3 shows an autoradiograph of a coronal section from this experiment in which two callosal columns and portions of an electrode track are visible. The sequence of binaural responses obtained during the penetration is illustrated below the autoradiograph. In this figure summation responses are indicated by '+'s and contralateral dominant suppression responses are indicated by 'C−'s. Moving from right to left, the electrode encountered alternating series of summation and contralateral dominant suppression responses. Such a sequence of binaural responses reflects the electrode's

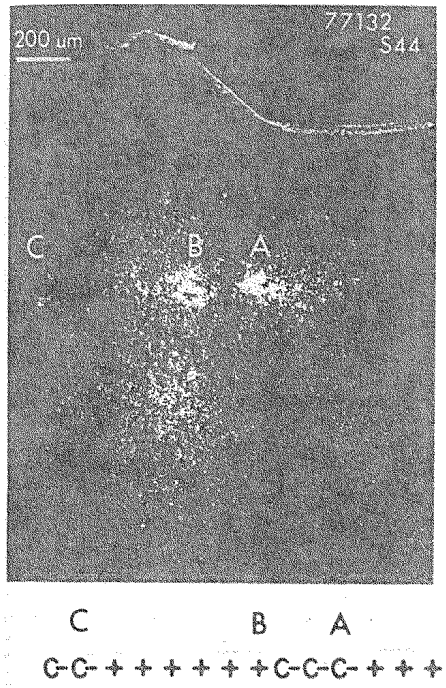

Fig. 3 Relationship between binaural and callosal columns seen in an autoradiograph of a coronal section through AI. Ten μCi of [^{3}H]-proline was injected at one site in AI of the right hemisphere. Beginning ten hours later, response properties of neurons were studied at 100-μm intervals during an electrode penetration oriented nearly parallel to the cortical laminae in AI of the left hemisphere. Marking lesions (labeled A, B and C) were placed at the borders of binaural columns. Sequence of binaural responses and lesions are shown below the photomicrograph. See text for description of binaural responses. Dorsal is toward the right. Best frequencies ranged between 12 and 13 kHz in the portion of the penetration that is illustrated.

passage through alternate summation and contralateral dominant suppression columns. During the electrode penetration three small electrolytic lesions were placed near binaural column borders and these are labeled *A*, *B*, and *C* in the autoradiograph and above the sequence of binaural response symbols. Lesions *A* and *B* in addition to corresponding with binaural column borders also appear to lie near the borders of callosal columns. Summation columns located between lesions *B* and *C* and to the right of lesion *A* appear more heavily labeled than the contralateral dominant suppression column located between lesions *A* and *B*. In the experiment illustrated in figure 4, 20 μCi of [^{3}H]-proline was injected into each of 35 locations in AI of the right hemisphere in order to label callosal fibers originating throughout the high-frequency representation. Injection sites were spaced at 1-mm intervals in a rectangular array covering the dorsal portion of the middle ectosylvian gyrus. A series of callosal columns and the track of an electrode which passed nearly parallel to the cortical laminae are clearly visible. Alternate series of contralateral dominant suppression responses (−) and summation responses (+) reflect the passage of the electrode through alternate binaural columns. The positions of marking lesions are labeled by the letters *A* through *E* in the photomicrograph and in the sequence of binaural response symbols. Inspection of the autoradiograph reveals that like the previous experiment each lesion lies near callosal and binaural column borders. The results of this experiment and the one previously described suggest that summation columns receive more dense callosal innervation than contralateral dominant suppression columns.

These findings are confirmed and extended to two other types of binaural responses in the experiment illustrated in figure 5. As in the last experiment callosal columns were labeled using multiple injections of [^{3}H]-proline. Sequences of binaural responses obtained in each of four electrode penetrations into AI along with a photograph of the autoradiograph containing each electrode track appear in figures 5A through D. Marking lesions placed during these electrode penetrations are designated by letters. Examples of heavily labeled summation columns are found between lesions *A* and *B* and between lesions *C* and *D* in figure 5a, between lesions *A* and *B* in figure 5B, to the right of lesion *B* and between lesions *C* and *D* in figure 5C and to the right of lesion *A* and between lesions *B* and *C* in figure 5D. Examples of relatively sparsely labeled contralateral dominant suppression columns are found between lesions *B* and *C* and between lesions *D* and *E* in figure 5A, to the left of lesion *B* in figure 5B, between lesions *B* and *C* and to the left of lesion *D* in figure 5C, and between lesions *A* and *B* in figure 5D.

Monaural contralateral (MC) responses were encountered in the penetration illustrated in figure 5A near lesion *D*. Although these appear interspersed with contralateral

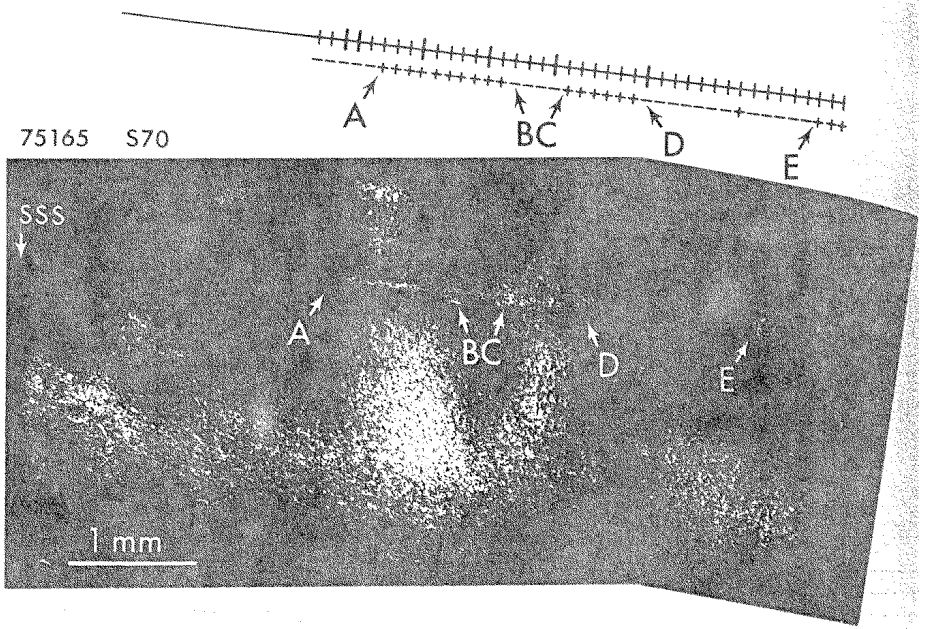

Fig. 4 Relationship between binaural and callosal columns seen in an autoradiograph of a coronal section through AI. Twenty μCi of [^{3}H]-proline was injected at each of 35 sites in AI of the right hemisphere. Six days later response properties of neurons were studied at 100-μm intervals during an electrode penetration that was oriented nearly parallel to the cortical laminae of AI of the left hemisphere. Marking lesions (labeled A through E) placed at the borders of binaural columns are shown in both the autoradiograph and the sequence of binaural response symbols. Light vertical bars indicate responses of neuron clusters. Heavy bars indicate responses of single neurons. Dorsal is toward the left. Best frequencies in this penetration dropped from 18 kHz near the beginning to 12 kHz near the end.

dominant suppression responses, they occur in a relatively sparsely labeled region and the border of a callosal column corresponds closely with the initial occurrence of the monaural contralateral responses. A monaural contralateral response also occurred between two series of summation responses between lesions *C* and *D* in figure 5A. Although this response did not coincide with a clearly defined callosal column border, it did occur in a region of relatively light labeling. These data suggest that like contralateral dominant suppression neurons, monaural contralateral neurons are found in areas which are relatively sparsely labeled.

Ipsilateral dominant suppression responses (I−) were encountered in penetrations illustrated in figures 5A and C. In figure 5A, these were the first two responses encountered in the penetration and are located to the right of lesion *A*. In figure 5C they are interspersed with summation responses and are located between lesions *A* and *B*. In both cases, ipsilateral dominant suppression responses, like summation responses, are found in cortical regions which are relatively densely labeled.

Although most binaural column borders appear to coincide with well defined callosal column borders, some do not. During the experiment illustrated in figure 5, 12 lesions were placed near the borders between summation and contralateral dominant suppression columns. Of these, eight lie on the borders of clearly defined callosal columns (i.e., lesions *B* and *C* in fig. 5A, lesion *B* in fig. 5B, lesions *B* and *D* in fig. 5C, and lesions *A*, *B* and *C* in fig. 5D). Some of the remaining four lesions also appear to correspond with less clearly defined callosal column borders. Lesion *E* in figure 5A was placed on a border between binaural col-

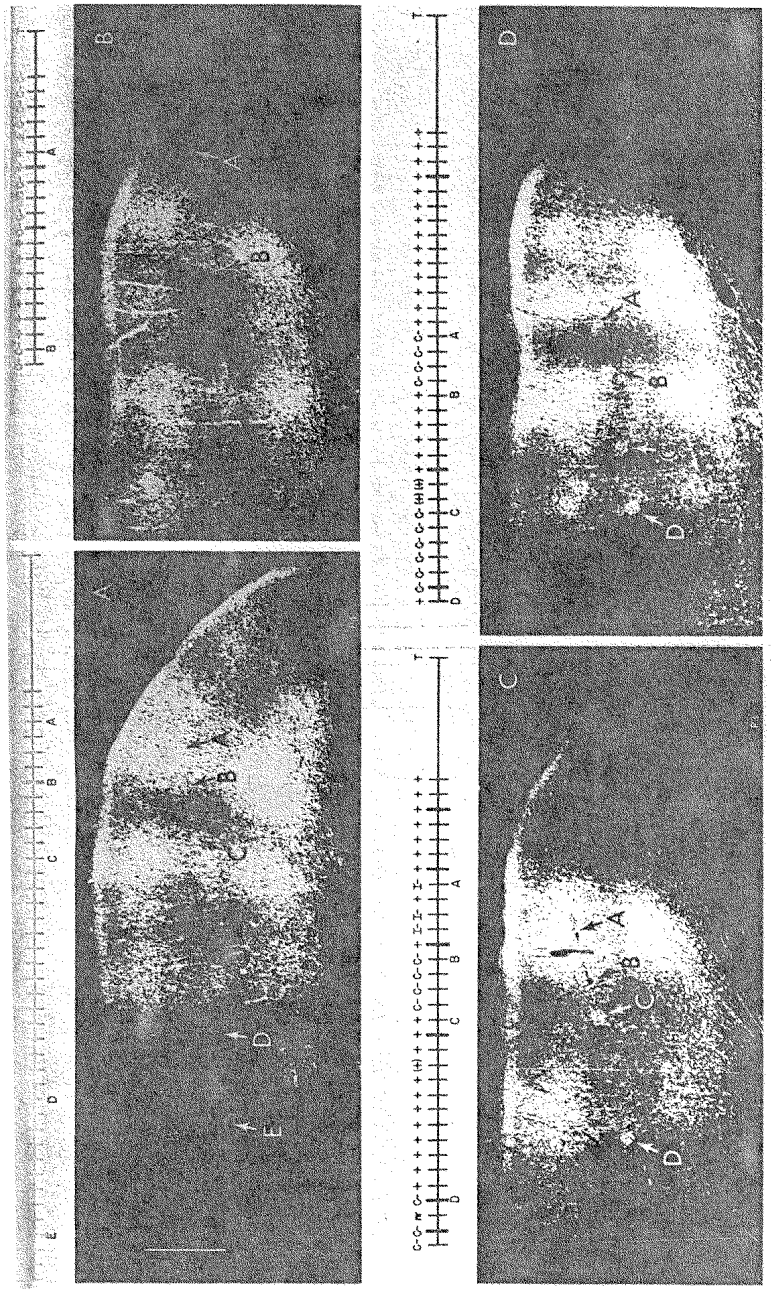

Fig. 5 Relationship between callosal columns and binaural responses encountered during four electrode penetrations through AI. Ten μCi of [^{3}H]-proline was injected into each of 27 sites in AI of the right hemisphere. Seven days later response properties of neurons were studied at 100-μm intervals during electrode penetrations oriented nearly parallel to the cortical laminae of AI of the left hemisphere. The locations of marking lesions are indicated by letters. Light vertical bars indicate responses of clusters of neurons. Heavy vertical bars indicate responses of single neurons. Each tissue section is oriented with the suprasylvian sulcus (dorsal) toward the right. During each electrode penetration, best frequencies decreased as the electrode moved from dorsal to ventral through AI. Best frequencies encountered in A decreased from 23 kHz to 9.5 kHz; in B from 15.8 kHz to 10.1 kHz; in C from 10.5 kHz to 4.9 kHz; and in D from 11.2 kHz to 7.5 kHz. Parentheses indicate poor responses.

umns in a region in which callosal columns were only faintly labeled. Nevertheless, a puff of silver grains in layer III of the summation column to the left of the lesion suggests that this lesion also lies on the border of a callosal column. In figure 5C, lesion *C* lies on a border between binaural columns and corresponds with a faint but noticeable change in the density of labeling of layers III and VI. Lesion *A* in figure 5B lies outside the region in which significant numbers of silver grains were found. Thus, of the 12 lesions placed on physiological borders between binaural columns, 11 were placed in regions where labeling of callosal afferents was sufficiently heavy to define callosal columns. Of these, eight lie on well defined callosal column borders and another two on somewhat less well defined borders. The remaining one, lesion *D* in figure 5D, does not coincide with a callosal column border.

Often the density of callosal labeling is not uniform in a binaural column. The summation column located between lesions *C* and *D* of figure 5C exhibits a clear gradient in the density of labeling and is much more heavily labeled at its left edge than at its right. In figure 5D, the summation column to the right of lesion *A* is less densely labeled in its center than at its periphery. Finally in figure 5A, the two summation columns located between lesions *C* and *D* and separated by a monaural contralateral response are more lightly labeled at their borders adjacent to the monaural contralateral response than at their far borders. Nonuniform labeling was not restricted to summation columns. The contralateral dominant suppression column located between lesions *C* and *D* in figure 5D is not uniformly labeled. Near lesion *C*, it is only lightly labeled but near lesion *D*, it is as heavily labeled as the summation column located at that lesion. Whether the nonuniform distribution of silver grains in binaural columns reflects a nonuniform distribution of callosal axon terminals or simply reflects nonuniform labeling of AI in the opposite hemisphere as a result of the multiple injection technique remains an open question.

Topography of callosal columns related to binaural and frequency maps of AI

Although the topography of binaural columns has not been described in detail, at least some columns appear as elongated strips which cross several octaves of the frequency representation. If callosal columns are related to binaural columns in the manner described above, one might expect to find a similar topographic pattern formed by callosal axon terminals. The results presented below confirm these expectations.

The topographic pattern of callosal columns is best appreciated in tissue sections cut parallel to the cortical surface. To obtain tissue sections cut in this plane, the cerebral hemisphere was gently pressed between two glass plates to flatten the gyral surfaces upon which auditory cortex is located. Tissue sections were then cut parallel to the flattened cortical surface. Figure 6 shows dark field photomicrographs of tissue sections from the right hemispheres from two brains cut in this plane. Callosal axon terminals were labeled by injecting [^{3}H]-proline at multiple sites in AI of the opposite hemisphere in the experiment illustrated in figure 6A. To insure that the pattern of terminal labelling obtained using the autoradiographic technique did not simply reflect nonuniform labeling in the injected hemisphere, the corpus callosum was sectioned in other experiments and the degenerating axons and axon terminals stained using the technique described by Fink and Heimer ('67). Figure 6B represents a tissue section from such an experiment. In both cases, light areas represent high concentrations of callosal axon terminals and dark areas represent low concentrations.

The topographic pattern of callosal columns exhibits certain consistent features in each of the six hemispheres that were studied. Whereas in coronal section dense aggregates of callosal axon terminals appeared as columns, in sections cut parallel to the cortical surface they take on more complex forms. Two prominent elongated callosal columns (α and β in fig. 6) run in a rostrodorsal to caudoventral direction through AI. Caudal to α and β callosal axon terminals are more uniformly distrib-

Fig. 6 Topographic distribution of callosal axon terminals seen in tissue sections cut parallel to the cortical surface which had been flattened by gently pressing it onto a glass plate.

A Autoradiograph of a tissue section in which callosal axon terminals were labeled with [^{3}H]-proline. One day prior to sacrifice, 20 μCi of [^{3}H]-proline was injected into each of 37 sites of the left hemisphere.

B Photomicrograph of degenerating callosal axon terminals which were stained using the procedure described by Fink and Heimer ('67). One week prior to sacrifice, the corpus callosum was completely sectioned using sterile surgical techniques.

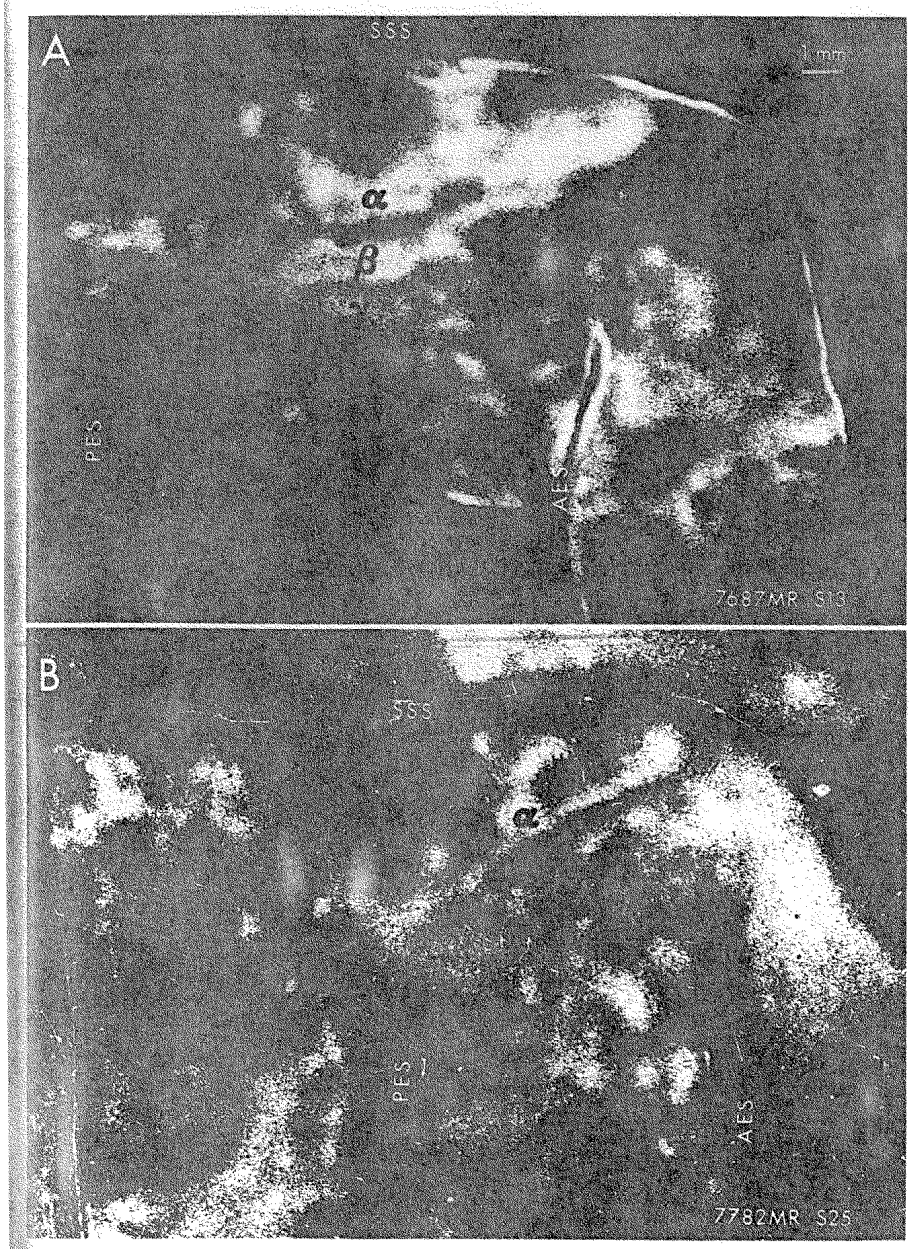

Figure 6

uted. The dorsal border of α is somewhat irregular and one or more branches extend toward and may enter the suprasylvian sulcus. Within α, callosal terminals are more densely concentrated than anywhere else in AI. The second highest concentration of terminals appears to be found in β. In the region labeled γ, callosal terminals are more uniformly distributed than above, but callosal columns are still evident. The lowest concentration of callosal terminals is found in the dark regions above and below α. In autoradiographs of tissue sections cut coronally, there is also some suggestion that callosal columns near the suprasylvian sulcus are formed by more dense accumulations of axon terminals than are those located lower in AI (figs. 4, 5). Above the upper end of the posterior ectosylvian sulcus is a region of sparse callosal innervation (fig. 6B). Rostral and ventral to this sparsely innervated region is α. Caudal to it in the dorsocaudal corner of the posterior ectosylvian gyrus is another complex of densely labeled callosal columns. Below γ near the anterior ectosylvian sulcus there often appears a complex of densely labeled callosal columns. Callosal columns are also found on the posterior and anterior ectosylvian and suprasylvian gyri. There are many individual differences in these patterns. For example, α and β may merge rostrally (fig. 6A) or caudally (fig. 6B), or may not merge at all (fig. 8A). In figure 8C, α and β appear to be composed of a series of smaller callosal columns but this pattern may reflect nonuniform labeling of callosal afferents by the multiple injection technique. The patterns described here occur in all tissue sections regardless of the cortical layers through which they pass. In spite of these and other differences between brains, the similarities between them remain impressive.

The patterns of callosal columns seen in figure 6A correspond closely with the map of binaural responses obtained in the same hemisphere (fig. 7). Lesions *A, C, D, E, F, H* and *K* were each placed on borders between binaural columns and each corresponds closely with the border of a callosal column. Within densely labeled regions, summation (+) responses were almost invariably encountered. Three electrode penetrations entered α. During their traverses, i.e., between lesions *A* and *C*, dorsal to the monaural contralateral (MC) responses encountered near lesion *H*, and ventral to lesion *K*, all neurons displayed summation with the exception of those located at lesion *G* which displayed ipsilateral dominance and suppression (I−). Two electrode penetrations passed through β. Between lesions *D* and *E* and between lesions *H* and *I*, all neurons displayed summation. Finally, one penetration passed through a callosal column located in γ (between lesions *E* and *F*) and here summation responses were also encountered. Within sparsely labeled regions, either contralateral dominant suppression or monaural contralateral responses were encountered. Above α between lesions *J* and *K*, contralateral dominant suppression (C−) responses were found. Two penetrations passed through the sparsely labeled band separating strip α and β and here, between lesions *C* and *D*, contralateral dominant suppression responses were found. Also in this sparsely labeled band above lesion *H*, monaural contralateral (MC) responses were found. Even in the sparsely labeled regions in γ (near lesions *E* and *F*) contralateral dominant suppression responses were found. Thus, these results provide further evidence that regions in which summation responses are encountered receive more dense callosal innervation than do regions in which contralateral dominant suppression or monaural contralateral responses are encountered.

The relationship between the pattern of callosal columns and the frequency map of AI is illustrated in figure 8. Dark field photomicrographs in the left column and frequency maps in the right column were derived from tissue sections cut parallel to the flattened cortical surface. Partial section of the corpus callosum in one cat resulted in the patterns of degenerating callosal axon terminals in both hemispheres which are illustrated in figures 8A and B. Rows of bright spots represent fiber degeneration produced by marking lesions placed during the mapping experiments. Electrode penetrations in which no marking lesions were placed did not result in noticeable

Fig. 7 Relationship between binaural and callosal columns in an autoradiograph of a tissue section cut parallel to the flattened cortical surface of AI. Following [^{3}H]-proline injections in the left hemisphere (see legend of fig. 6 for details) the responses of neurons were studied in 100-μm intervals in penetrations oriented parallel to the cortical laminae in AI of the right hemisphere. The locations of marking lesions (labeled A through K) placed during three electrode penetrations (labeled 1, 2 and 3) are shown in both the autoradiograph and the sequences of binaural response symbols. Best frequencies (in kHz) obtained at points where lesions were placed are indicated beneath letters in the symbol sequence.

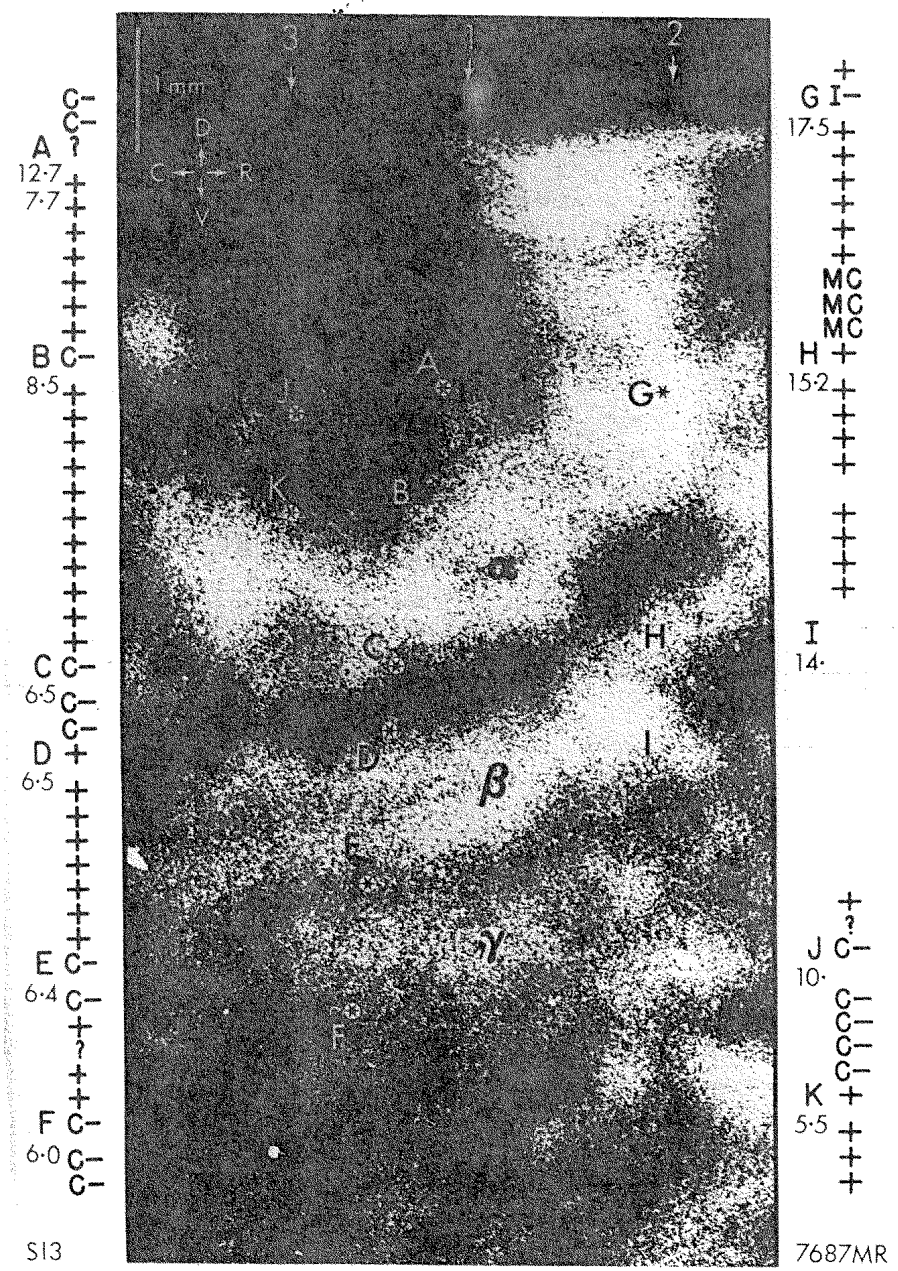

Figure 7

fiber degeneration. Callosal axon terminals were labeled by multiple injections of [^{3}H]-proline in the experiment illustrated in figure 8C.

Elongated callosal columns appear to cross several octaves of the frequency representation in AI. Stippling on the frequency maps in figure 8 represents the locations and configurations of some of the most prominent accumulations of callosal axon terminals which appear in the corresponding photomicrographs. On each map both α and β are shown. The lower border of α, all of β and the sparsely innervated zone between α and β appear roughly parallel and cross perpendicular to isofrequency contours (dotted lines in fig. 8). A similar relation was found in the experiment illustrated in figure 7. Best frequencies obtained at each marking lesion are shown on the sides of the photomicrograph. Best frequencies near 6 kHz were obtained at lesions *K, C, D, E* and *F*. These lesions define an isofrequency contour which is oriented nearly perpendicular to the elongated patches. Ventral to β (in the region corresponding to γ in fig. 6) lower concentrations of callosal terminals are found and here the relation between the frequency map and callosal columns is less clear. Although there is a suggestion of elongated callosal columns in this region in two brains (figs. 7, 8C), in others there is not (figs. 6B, 8A,B).

The dorsal and ventral borders of AI appear to be related to the pattern of callosal columns within the high frequency representation. The major portion of α and its dorsally directed branches appear to lie within AI. In the region dorsal and caudal to α neurons often have best frequencies which do not correspond with the frequency organization of AI (figs. 8B,C). The border between AI and AII appears to lie in a zone of relatively sparse callosal innervation (γ in fig. 6). Thus α, β and γ appear to coincide with the dorsoventral extent of AI.

Elongated callosal columns extend to the rostral border of AI. Rostral to AI lies the anterior auditory field (Knight, '77). Its high frequency representation adjoins that of AI and lower frequencies are located rostroventrally (figs. 8A,B). The densely labeled strip formed by the union of α and β in figure 6A appears to cross the rostral border of AI into the anterior auditory field. In figure 8A, α and β do not appear to cross into the anterior auditory field, but elongated callosal columns are present in the anterior auditory field. α and β extend to the rostral border of AI and merge in figure 8B. The border between AI and the anterior auditory field was not defined in figure 8C.

Although our material suggests that elongated callosal columns extend to the high-frequency border of AI, the lower end of the frequency range covered appears more variable. In figure 6, α and β extend into the frequency representation below 6.5 kHz (lesions *C* and *D*) and probably fade out around 4 kHz. Likewise α and β in figure 8C and α in figure 8B fade out around 5 to 6 kHz. β in figures 8A and B probably does not reach lower than 15 kHz. The corpus callosum was incompletely sectioned in the brain from which figures 8A and B were derived. It is conceivable that β appears rather short because some of its callosal innervation remained intact. In spite of some variability our data suggest that elongated callosal columns are found within the frequency representation between 4 and 45 kHz.

All portions of the frequency representation receive callosal input. We have observed callosal columns throughout the frequency representation from 90 Hz to 45 kHz. The tissue section illustrated in figure 2B lies within 300 μm of an electrode penetration in AI in which neurons with best frequencies below 100 Hz were encountered. Labeling of callosal terminals can clearly be seen in this region. Nevertheless, elongated patches in figure 6 and figure 8 (with the exception of α in fig. 8C) appear to stop short of entering the posterior ectosylvian sulcus which contains the low-frequency representation. Our material is not cut in a suitable plane to determine if the topography of callosal columns is related to the frequency map in the low-frequency representation.

AI neurons giving rise to callosal axons

In order to study the distribution of AI neurons that give rise to callosal efferents, the HRP technique of retrograde axoplasmic transport was utilized. In three experiments, a solution of HRP was injected at multiple locations into AI. Following histological processing, cells that contained granules of HRP reaction product were found in AI contralateral to the injected hemisphere.

Several morphologically distinct types of neurons located in cortical laminae III through VI were labeled as a result of this procedure. No labeled cells were found in layers I

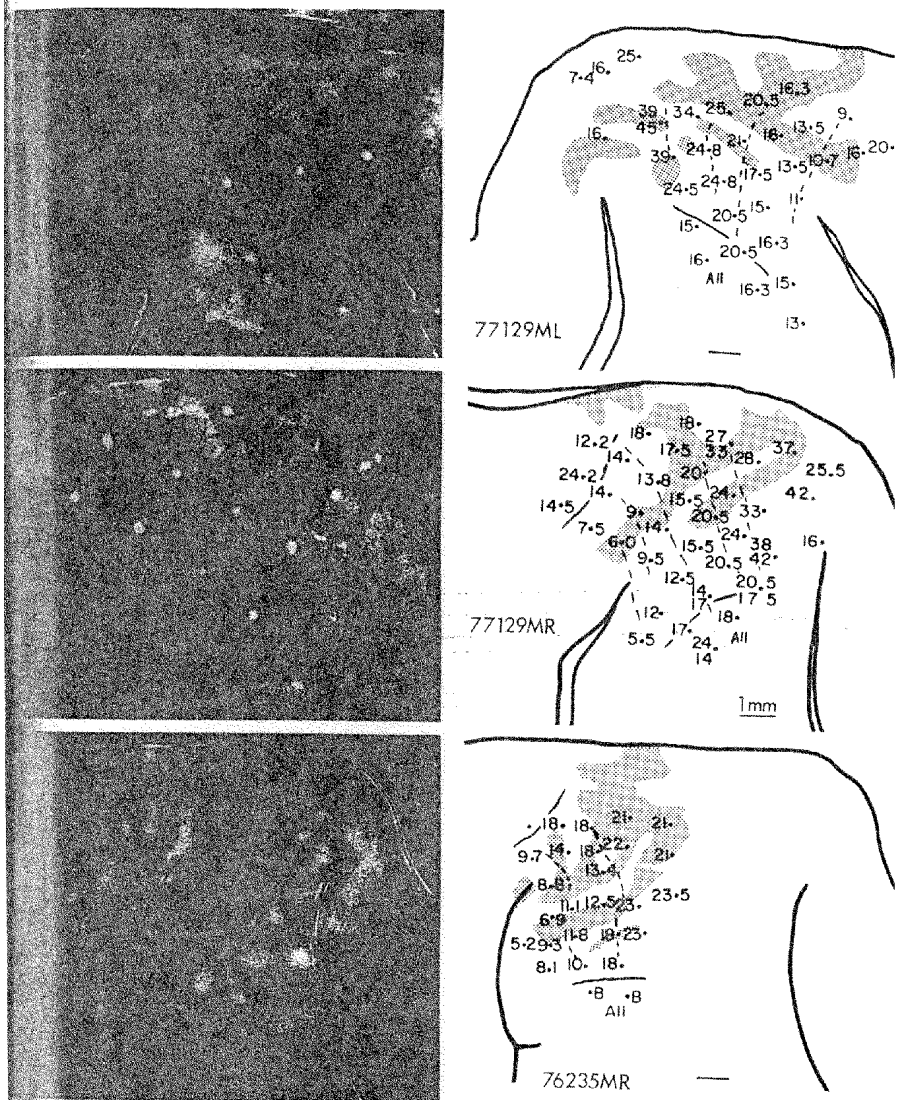

Fig. 8 Topography of callosal columns related to frequency maps in tissue sections cut parallel to the flattened cortical surface. Stippling on the frequency maps indicates positions and configurations of major callosal columns which appear in the corresponding frequency maps. Best frequencies are expressed in kHz. Decimal points represent the positions of electrode penetrations. Portions of the ventral border between AI and AII and the dorsocaudal border of AI are represented by heavy lines in frequency maps.

A,B One week following section of the caudal half of the corpus callosum, electrophysiological maps of each hemisphere were obtained. Following the experiment degenerating axon terminals were stained using the procedure described by Fink and Heimer ('67). Arrays of light spots in photomicrographs represent fiber degeneration caused by marking lesions.

C Ten μCi of [^{3}H]-proline was injected into each of 107 locations in auditory cortex of the left hemisphere. The following day the right hemisphere was mapped.

and II. In the lower two-thirds of layer III and scattered throughout layer IV labeling was restricted exclusively to pyramidal cells. Of 3,659 labeled cells counted in layers III through VI, 94% were pyramidal cells located in layers III and IV. A dense aggregation of labeled cells in these layers may be seen in the upper third of figure 9B. The density of labeling varied among cells and it was not uncommon to find densely labeled profiles adjacent to sparsely labeled ones. When viewed at greater magnification (fig. 9C), granules of the HRP reaction product may be seen to invade the proximal portions of the apical and basal dendrites. One striking feature of the labeled neurons in layers III and IV is their nonuniform distribution. Often labeled cells aggregate into clusters. In figure 10A, labeled cells are represented as dots on a drawing of a tissue section and clusters of cells may be seen in layers III and IV. In other tissue sections, however, clustering was less pronounced.

The remaining 6% of the labeled cells were found in layers V and VI. In figure 9B, the labeled pyramidal cells in layers III and IV are evident near the top of the photograph. Near the bottom two labeled cells are seen in layer VI (arrows). These appear at higher magnification in figure 9I. Other examples of labeled cells found in layer VI are illustrated in figures 9F, G and H. These cells tend to be spindle shaped with a single stained apical dendrite. The morphology of the basal dendrites, as revealed by HRP staining, is more varied. The cells illustrated in figures 9F and G each have a single basal dendrite. In figure 9F the basal dendrite bifurcates shortly after leaving the cell body but in figure 9G, no branching is apparent. The cell illustrated in figure 9H on the other hand has two basal dendrites. Layer V contains somewhat fewer labeled cells than does layer VI. Two examples of labeled profiles found in layer V are illustrated in figures 9D and E. Two labeled cells in figure 9D each have multiple apical dendrites and a single basal dendrite. In figure 9E, a labeled pyramidal cell in layer V has a single apical dendrite and multiple basal dendrites.

Distribution of callosal efferent neurons related to binaural columns

The presence of clusters of labeled cells in layers III and IV suggested that labeled cells might be more densely aggregated in certain binaural columns than others. To test this hypothesis, injections of HRP into AI of one hemisphere were combined with electrophysiological mapping of binaural columns in the other. Figure 9A is a photograph of a tissue section which was processed using the HRP method. In this figure, a marking lesion (L) is visible at the border between a contralateral dominant suppression column on the left and a summation column on the right. Identification of labeled cells in this photograph is somewhat obscured by artifacts present in the tissue section, but careful inspection reveals that there are many more labeled profiles in the summation column on the right side of the lesion than in the contralateral dominant suppression column on the left. Although several examples suggested that labeled cells were more densely aggregated in summation columns than in contralateral dominant suppression columns, in many cases, visual inspection of tissue sections alone did not reveal dramatic differences in the packing density of labeled cells between neighboring binaural columns.

To determine with greater confidence whether labeled cells were more densely aggregated in certain binaural columns than others, we chose to count the number of labeled neurons in a narrow column of cortical tissue whose sides were parallel to radial cell columns. We refer to these tissue columns as *sectors*. One sector is outlined by interrupted lines in the tissue section drawing in figure 10A.

The histograms in figure 10 illustrate the relation between cell counts per sector and the binaural response characteristics of neurons

Fig. 9 AI callosal efferent neurons labeled with HRP. HRP (0.5 μl of a 33% solution) was injected into each of 35 locations in AI of the right hemisphere. Later, binaural properties of neurons were studied at 100-μm intervals during electrode penetrations oriented nearly parallel to the cortical laminae in AI of the left hemisphere.

A A marking lesion (L) is visible which was placed near the border between a summation column (on the right) and a contralateral dominant suppression column (on the left). More labeled cells are visible to the right of the lesion than to the left.

B Labeled cells located in layers III and IV are visible near the top of this photograph. Near the bottom, arrows indicate the location of two labeled cells in layer VI.

C Labeled cells in layer III.

D,E Labeled cells in layer V.

F-H Labeled cells in layer VI.

I Labeled cells in layer VI which are also visible in the lower part of figure B.

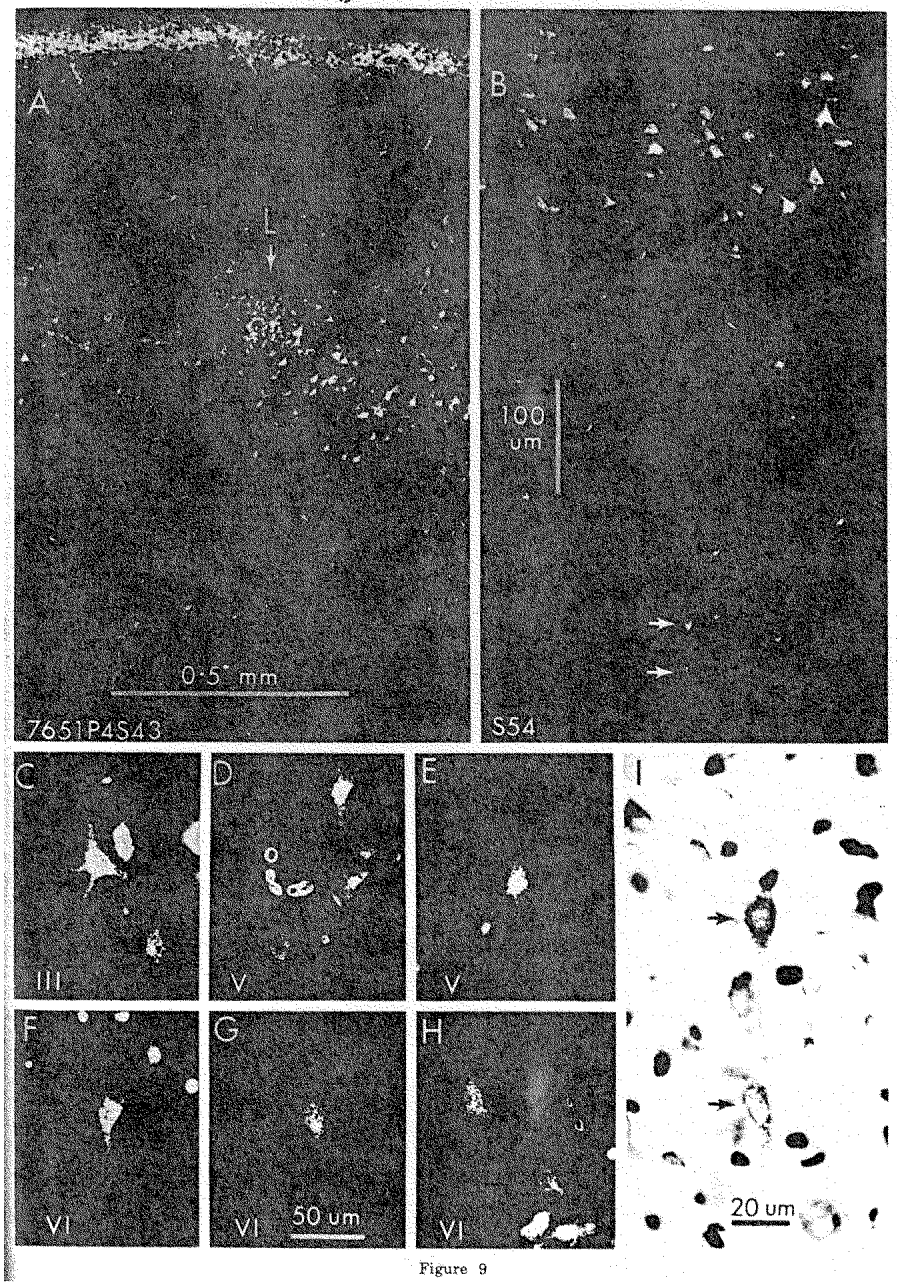

Figure 9

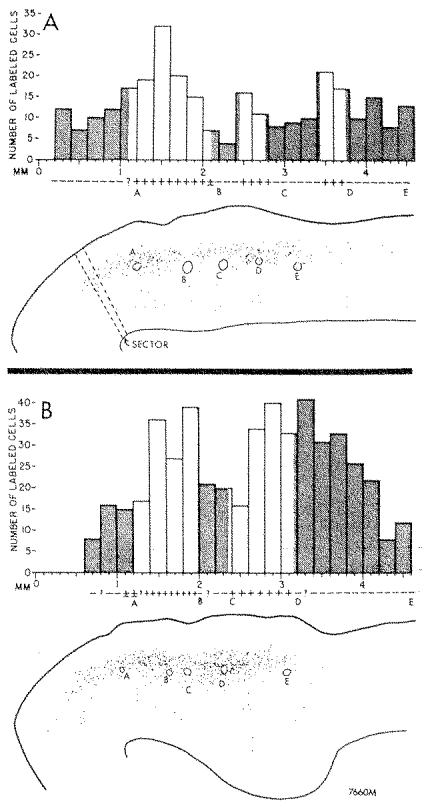

Fig. 10 Numbers and distributions of AI neurons giving rise to callosal fibers related to binaural properties of neurons. HRP (0.5 μl of a 40% solution) was injected into each of 36 locations in AI of the right hemisphere. Later, binaural responses of neurons were studied at 100-μm intervals during electrode penetrations which were oriented nearly parallel to the cortical laminae in AI of the left hemisphere. Marking lesions (labeled A through E) were placed near binaural column borders. Tissue sections were cut in the coronal plane. Dorsal is toward the left. Each labeled cell is represented as a dot in each drawing. Sectors have cross sectional dimensions of 180 × 200 μm. Borders of one sector are indicated by interrupted lines in A. Each histogram bin represents the number of labeled cells in a sector. Shaded bins represent sectors containing contralateral dominant suppression neurons. Open bins represent sectors containing summation neurons. In the penetration illustrated in A, best frequencies ranged from 16 kHz near the beginning of the penetration to 10 kHz at the end. The penetration illustrated in B was located about 1 mm posterior to that illustrated in A and best frequencies ranged from 16.5 kHz near the beginning of the penetration to 7.4 kHz at the end.

located within those sectors. Each bin in the histogram represents the number of labeled cells in one sector and adjacent bins represent adjacent sectors. Below each histogram is plotted the sequence of binaural responses obtained in an electrode penetration which was oriented nearly parallel to the cortical laminae. The electrode passed through the center of each sector from which the cell counts in the histograms were obtained. Binaural properties are plotted in registration with the abscissa of the histogram using the marking lesions as reference points for both sets of data. The outlines of marking lesions and the locations of labeled cells are represented in the drawings below each histogram.

The nonuniform distribution of labeled cells in layers III and IV is reflected as peaks and valleys in the histograms. For ease of relating cell counts to binaural response properties, bins representing sectors located in contralateral dominant suppression columns have been shaded. Sectors which cross binaural column borders (e.g., the fifth bin from the right in fig. 10A) are partially shaded. In figure 10A, the electrode passed through three summation columns (series of '+'s) and each column corresponds with a peak in the histogram. Likewise, each of the four contralateral dominant suppression columns (series of '−'s) penetrated by the electrode corresponds with a valley in the histogram. The results from a second penetration in the same experiment are illustrated in figure 10B. Between lesions *C* and *E*, the tissue section is cut obliquely with respect to radial cell columns. Consequently, in this region, cell counts were not obtained from sectors but instead from tissue columns whose sides were not parallel to radial cell columns. Because in this instance cell counts do not represent the number of labeled cells in the radial column from which binaural responses of neurons were obtained, we restrict consideration to the portion of the tissue section to the left of lesion *C* which was cut parallel to the radial alignment of cells. Here, the peak in the histogram corresponds with a summation column and the valleys which flank the peak correspond with contralateral dominant suppression columns. The results obtained from both penetrations suggest that sectors located in summation columns contain greater numbers of callosal efferent cells than do sectors located in contralateral dominant suppression columns.

Histograms in figure 11 illustrate the results obtained from another experiment and relate counts of labeled cells to binaural columns. As seen in figure 10, peaks and valleys in the histograms reflect the non-uniform distribution of labeled cells in layers III and IV. Cell counts obtained from sectors containing contralateral dominant suppression (−) or monaural contralateral (MC) neurons are represented by shaded bins in the histograms. Contralateral dominant suppression responses in general tend to correspond with valleys of the histograms and examples are located near lesions *A*, *B* and *D* in figure 11A, near lesions *B*, *C* and *D* in figure 11B and near lesion *C* in figure 11C. A series of monaural contralateral (MC) responses to the right of lesion *C* in figure 11A also appears to correspond with a valley in the histogram. Cell counts obtained from sectors located in summation columns (responses indicated by '+'s) are represented by open bins and these, in general, correspond with peaks in the histograms. Examples of these are located between lesions *A* and *B*, between lesions *B* and *C* in figure 11A, between lesions *B* and *C* and between lesions *C* and *D* in figure 11B, and between lesions *A* and *B* in figure 11C. Furthermore, in two penetrations, ipsilateral dominant suppression (I−) responses were encountered. Histogram bins corresponding with these responses are distinguished by diagonal lines. Between lesions *A* and *B* in figure 11B and between lesions *A* and *B* in figure 11C, ipsilateral dominant suppression responses correspond with peaks in the histograms. In general, the results obtained in the experiments illustrated in figures 10 and 11 suggest that sectors in which summation or ipsilateral dominant suppression neurons are found contain more labeled cells than do sectors in which contralateral dominant suppression or monaural contralateral neurons are found. These data also suggest that the sources of callosal axons may be more heavily concentrated in summation columns located dorsally in AI than those located more ventrally.

Careful inspection of the histograms in figures 10 and 11 reveals certain examples which do not fit the general relationship outlined above. Perhaps the most striking example is the summation response located at lesion *A* in figure 11C which corresponds with the lowest bin value in the histogram, a finding counter to the general trend. Furthermore, neither the summation column near lesion *E* in figure 11B nor the suppression column near lesion *B* in figure 11C corresponds with a clear peak or valley in the histogram. Finally, even in regions where there is apparently a good correspondence between histogram peaks and valleys and binaural columns (e.g., between lesions *A* and *C* in figure 11A), some sectors in contralateral dominant suppression columns contain more labeled cells than sectors in summation columns.

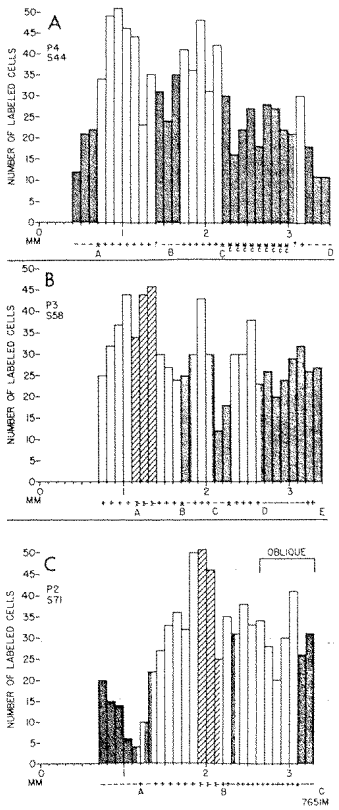

Fig. 11 Numbers and distributions of AI neurons giving rise to callosal fibers related to binaural properties of neurons. Positions of marking lesions (labeled A through E) are shown in the sequences of binaural response symbols. Penetrations are oriented as in figure 10. Each histogram bin represents the number of labeled cells per sector. Shaded bins represent sectors containing contralateral dominant suppression and monaural contralateral neurons. Open bins represent sectors containing summation neurons. Bins with diagonal lines represent sectors containing ipsilateral dominant suppression neurons. Sectors had cross sectional dimensions of 180 × 100 μm at the III-IV border. Electrode penetrations were approximately parallel and spaced about 1 mm apart. The penetration illustrated in A was located most rostral, that in C most caudal. In A, best frequencies decreased from 18 kHz near the beginning of the penetration to 14.5 kHz near the end; in B from 16.5 kHz to 9 kHz; and in C from 13 kHz to 5 kHz. In C, OBLIQUE indicates that the tissue section in this region was cut oblique with respect to radial cell columns. For details of the HRP injection see legend of figure 9.

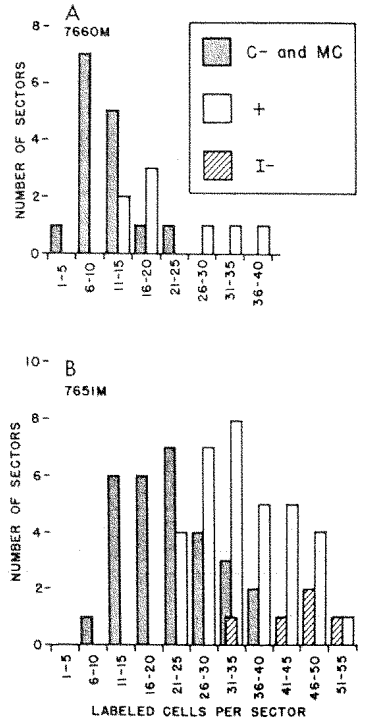

Fig. 12 Distributions of cell counts per sector related to binaural properties of neurons. Each histogram includes all sector values obtained in one experiment except those from sectors in which the binaural properties of neurons varied or those from sectors which were located in regions in which the cortex was cut oblique with respect to radial cell columns. Shaded bins represent the distributions of cell counts obtained from sectors containing contralateral dominant suppression neurons (A) or contralateral dominant suppression and monaural contralateral neurons (B). Open bins represent the distribution of cell counts obtained from sectors containing summation neurons; diagonal lines designate bins representing the distribution of cell counts obtained from sectors containing ipsilateral dominant suppression neurons.

Distributions of cell counts obtained from regions that contain neurons with similar binaural properties are graphically represented in figure 12. These distributions include all sector values obtained during penetrations in one experiment except those from sectors which crossed binaural column borders or which were located in regions where the cortex was cut oblique with respect to radial cell columns. In figures 12A and B, values from experiments 7660M and 7651, respectively, are plotted. Shaded bins represent the distribution of cell counts obtained from sectors containing contralateral dominant suppression or monaural contralateral neurons. These values have been combined since a t-test did not reveal any significant difference between the two populations. Open bins represent the distribution of cell counts obtained from sectors containing summation neurons. Although the two distributions overlap, values obtained from sectors containing summation neurons in general exceed values obtained from sectors containing contralateral dominant suppression and monaural contralateral neurons. A t-test shows that the distributions are significantly different ($p < 0.001$). Bars that contain diagonal lines designate the distribution of cell counts obtained in regions containing ipsilateral dominant suppression neurons. Although few in number, these sectors contain significantly more labeled neurons than do sectors in which summation neurons are found (Mann Whitney U-test; $p < 0.033$). In summary, sectors containing contralateral dominant suppression or monaural contralateral neurons contain significantly fewer labeled cells than do sectors containing summation neurons. The greatest number of cells are found in sectors containing ipsilateral dominant suppression neurons.

From the mean number of labeled cells per sector and the cross sectional area of sectors, it is possible to estimate the number of labeled cells in a binaural column with a cross sectional area of one square millimeter. These computations reveal that fewer cells were labeled in experiment 7660M than in experiment 7651M. The number of labeled cells per square millimeter of summation column was estimated to be 614 in experiment 7660M and 1,987 in experiment 7651M. The number of labeled cells per square millimeter of contralateral dominant suppression column was esti-

mated to be 315 in experiment 7660M and 1,161 in experiment 7651M. The differences in cell counts in these experiments may reflect differences in staining as tissue sections from experiment 7660M were less intensely stained for the HRP reaction product than were those from experiment 7651M. Although the technique employed here is not adequate to produce a reliable estimate of the absolute number of callosal efferent neurons in different binaural columns, it may provide an estimate of the relative number of callosal efferent neurons in different binaural columns. In experiment 7660M, sectors located in summation columns contained 1.95 times as many labeled neurons as did sectors which were located in contralateral dominant suppression columns. In experiment 7651M, 1.76 times as many labeled neurons were found in sectors containing summation neurons as in sectors containing contralateral dominant suppression and monaural contralateral neurons. Sectors in which ipsilateral dominant suppression neurons were found contained 2.18 times as many labeled neurons as did sectors in which contralateral dominant suppression and monaural contralateral neurons were found. Although the difference in staining of tissue sections from these two experiments may be reflected dramatically in the absolute number of cells which are labeled, the relative number of labeled cells in different binaural columns is more constant between experiments.

DISCUSSION

A major finding of this study is the remarkable relation of the pattern of callosal connections to the sensory representations in the high-frequency portion of AI. Both the sources and terminations of callosal fibers are more densely aggregated in regions containing summation and ipsilateral dominant suppression neurons than in regions containing contralateral dominant suppression and monaural contralateral neurons. Thus, it appears that regions in AI which are the major contributors to the callosal pathway are also the major recipients.

The callosal innervation pattern is also related to the frequency organization of AI. Bands formed by dense or sparse concentrations of callosal axon terminals cross the high frequency representation roughly orthogonal to isofrequency contours. In a previous physiological study a contralateral dominant suppression column was mapped which occupied a strip of cortex that was oriented orthogonal to isofrequency contours (Imig and Adrián, '77); in the present study similar columns were seen to correlate with bands of sparse callosal innervation. The presence of elongated bands formed by dense concentrations of callosal fiber terminals suggests that elongated summation columns may also exist which are oriented orthogonal to isofrequency contours. Callosal axons also terminate in the low-frequency representation of AI but whether the pattern of innervation correlates with the binaural and frequency organization of this region is not known.

Although there is a clear correlation between the distributions of the sources and terminals of callosal axons and binaural organization in AI, callosal innervation does not appear to be necessary for binaural responsiveness of neurons in the primary field. Even in brains in which callosal input has been removed, neurons in AI remain binaurally responsive (Brugge and Imig, '78). It is likely that much of the binaural activity we have recorded in AI reflects binaural interactions in the brainstem where responses similar to those recorded from cortical cells have been reported (Boudreau and Tsuchitani, '68; Brugge et al., '70; Guinan et al., '72; Goldberg and Brown, '68; Rose et al., '66).

Summation and contralateral dominant suppression neurons have been shown by Imig and Adrián ('77) to form functional columns in AI. In that study and the present one, ipsilateral dominant suppression and monaural contralateral neurons were also encountered. These two classes of neurons may also form functional columns, although we have not encountered cells with these properties in sufficient numbers to study this aspect of their organization.

Earlier degeneration studies in cat, raccoon and monkey had shown variability in callosal innervation density within AI (Ebner and Myers, '65; Diamond et al., '68; Karol and Pandya, '71; Pandya et al., '69). The topographic pattern of callosal innervation of the auditory area in the rhesus monkey shows certain similarities to our findings in cat. Karol and Pandya ('71) found three parallel bands of dense callosal degeneration running longitudinally on the superior temporal plane. In the cat Ebner and Myers ('65) and Diamond et al. ('68) described several areas in and around AI that received only sparse callosal input. The most conspicuous of these regions lies above

the upper end of the posterior ectosylvian sulcus and rostral to a visually responsive region in the dorsocaudal tip of the posterior ectosylvian gyrus (Palmer et al., '78) that contains a complex of callosal columns. Diamond et al. ('68) suggested that this sparsely innervated region may correspond with the low- to mid-frequency representation of AI. Our combined electrophysiological and anatomical mapping data indicate that this region which is clearly seen in Fink-Heimer material lies outside of the primary field.

The relation between the pattern of callosal connectivity and the binaural representation in AI suggests that the callosal pathway may function to transmit a specific subset of information between the primary auditory fields. In experiments in which HRP was injected into AI, nearly twice as many labeled neurons were found in sectors containing summation or ipsilateral dominant suppression neurons than in sectors containing contralateral dominant suppression or monaural contralateral neurons. Thus, binaural information transmitted by the population of AI callosal cells differs from the binaural information transmitted by the general population of AI neurons.

The population of AI callosal neurons may also differ from the general population of AI neurons with respect to the transmission of other auditory information. An electrode penetration oriented more or less parallel to an isofrequency contour in the high-frequency representation of AI passes through several summation and several contralateral dominant suppression columns (figs. 3-5, 7, 10, 11). The spatial separation of groups of neurons with similar best frequencies and binaural properties may reflect the topographic representations of still other stimulus modalities, e.g., sound pressure level (Brugge and Merzenich, '73; Suga, '77) or direction of sound movement (Sovijärvi, '73; Sovijärvi and Hyvärinen, '74). A summation column located on the dorsal portion of an isofrequency contour appears to receive a higher concentration of callosal axon terminals than one located more ventrally. A contralateral dominant suppression column located on the dorsal portion of an isofrequency contour generally appears to be less densely innervated than one located more ventrally. A similar gradient in the distribution of the sources of callosal axons may obtain. Thus, if another stimulus modality is topographically represented along an isofrequency contour, then the representation of that modality in the population of AI callosal neurons may differ from its representation in the entire pool of AI cells.

Cortico-cortical pathways reciprocally connect AI with a number of other auditory fields in the same hemisphere. Each of these pathways may function to transmit a specific subset of auditory information. Axon terminals of these pathways are also distributed in patches in AI and other auditory fields (Imig and Reale, unpublished observations). How these different projection patterns overlap and the information transmitted over each of these pathways are problems currently under investigation in our laboratory.

Callosal fibers may connect together functionally related regions in primary visual and auditory cortices. Although the representation of the visual field in area 17 of the Siamese cat differs considerably from that in the normal cat, callosal fibers in both appear to connect together regions of area 17 in the two hemispheres that represent identical loci in the visual field (Berlucchi et al., '67; Choudhury et al., '65; Garey et al., '68; Hubel and Wiesel, '67; Shatz, '77a,b; Wilson, '68). The results of experiments which combined [^{3}H]-proline labeling of callosal fibers with electrophysiological mapping of AI in both hemispheres suggest that callosal fibers interconnect identical portions of the frequency representation in the two hemispheres (Brugge and Imig, '78; Imig and Reale, '77; Imig et al., '77). Whereas regions in AI that are the major contributors to the callosal pathway are also the major recipients, we have no direct evidence that regions of common binaural function are interconnected. Nevertheless, our findings are not incompatible with such a scheme. Most neurons in the high frequency representation of AI display one of three properties: they may be maximally excited by monaural stimulation to the left ear, by monaural stimulation to the right ear, or by binaural stimulation. Binaural stimulation maximally excites neurons in both hemispheres that are characterized by summation. If callosal fibers join functionally similar areas then regions containing summation neurons might be expected to be interconnected. Monaural stimulation, on the other hand, maximally excites the relatively small population of neurons displaying ipsilateral dominance and suppression in the hemisphere ipsilateral to the stimulated ear and the rel-

atively large population in the opposite hemisphere that comprises monaural contralateral and contralateral dominant suppression neurons (Imig and Adrián, '77). Regions containing ipsilateral dominant suppression neurons contain higher concentrations of sources and terminals of callosal axons than do regions containing monaural contralateral dominant suppression neurons. If these regions are interconnected, then one might expect that callosal neurons that are in relatively low concentration in monaural contralateral and contralateral dominant suppression areas might converge to densely innervate the much smaller area occupied by ipsilateral dominant suppression neurons. Conversely, callosal neurons that are in relatively high concentration in ipsilateral dominant suppression regions might diverge to innervate only sparsely the relatively large region occupied by monaural contralateral and contralateral dominant suppression cells. Although callosal fibers appear to interconnect functionally similar portions of the frequency representation, further study is necessary to determine if this is also true with respect to the binaural representation.

ACKNOWLEDGMENTS

We wish to express our appreciation to Elaine Langer, JoAnn Ekleberry, Joan Meister, Inge Siggelkow and Cathy Gooch for the histological work, to Shirley Hunsaker for photography and Sigrid Borgner for typing the manuscript. We also acknowledge Doctors Kathleen FitzPatrick and Richard Reale for participating in some of the experiments.

This work was supported by NSF Grant BNS76-19893, NIH Program Project Grant NS12732, and NIH Core Support Grant HD03352.

LITERATURE CITED

Aitkin, L. M., D. J. Anderson and J. F. Brugge 1970 Tonotopic organization and discharge characteristics of single neurons in nuclei of the lateral lemniscus of the cat. J. Neurophysiol., *33:* 421-440.

Berlucchi, G., M. S. Gazzaniga and G. Rizzolatti 1967 Microelectrode analysis of transfer of visual information by the corpus callosum. Arch. ital. Biol., *105:* 583-596.

Boudreau, J. C., and C. Tsuchitani 1968 Binaural interaction in the cat superior olive S segment. J. Neurophysiol., *31:* 442-454.

Brugge, J. F., D. J. Anderson and L. M. Aitkin 1970 Responses of neurons in the dorsal nucleus of the lateral lemniscus of cat to binaural tonal stimulation. J. Neurophysiol., *33:* 441-458.

Brugge, J. F., and T. J. Imig 1978 Some relationships of binaural response patterns of single neurons to cortical columns and interhemispheric connections of auditory area AI of cat cerebral cortex. In: Evoked Electrical Activity in the Auditory Nervous System. R. F. Naunton, ed. Academic Press.

Brugge, J. F., and M. M. Merzenich 1973 Responses of neurons in auditory cortex of the macaque monkey to monaural and binaural stimulation. J. Neurophysiol., *36:* 1138-1158.

Choudhury, B. P., D. Whitteridge and M. E. Wilson 1965 The function of the callosal connections of the visual cortex. Quart. J. Exptl. Physiol., *50:* 214-219.

Cowan, W. M., D. I. Gottlieb, A. E. Hendrickson, J. L. Price and T. A. Woolsey 1972 The autoradiographic demonstration of axonal connections in the central nervous system. Brain Res., *37:* 21-51.

Diamond, I. T., E. G. Jones and T. P. S. Powell 1968 Interhemispheric fiber connections of the auditory cortex of the cat. Brain Res., *11:* 177-193.

Ebner, F. F., and R. E. Myers 1965 Distribution of corpus callosum and anterior commissure in cat and raccoon. J. Comp. Neur., *124:* 353-366.

Fink, R. P., and L. Heimer 1967 Two methods for selective silver impregnation of degenerating axons and their synaptic endings in the central nervous system. Brain Res., *4:* 369-374.

Fisken, R. A., L. J. Garey and T. P. S. Powell 1975 The intrinsic, association, and commissural connections of area 17 of the visual cortex. Phil. Trans. Roy. Soc. Lond. B., *272:* 487-536.

Garey, L. J., E. G. Jones and T. P. S. Powell 1968 Interrelationships of striate and extrastriate cortex with primary relay sites of the visual pathway. J. Neurol. Neurosurg. Psychiatr., *31:* 135-157.

Goldberg, J. M., and P. B. Brown 1968 Functional organization of the dog superior olivary complex: an anatomical and electrophysiological study. J. Neurophysiol., *31:* 639-656.

Guinan, J. J., S. S. Guinan and B. E. Norris 1972 Single auditory units in the superior olivary complex. I. Responses to sounds and classifications based on physiological properties. Intern. J. Neurosci., *4:* 101-120.

Hubel, D. H., and T. N. Wiesel 1967 Cortical and callosal connections concerned with the vertical meridian of visual fields in the cat. J. Neurophysiol., *30:* 1561-1573.

Imig, T. J., and H. O. Adrián 1977 Binaural columns in the primary field (AI) of cat auditory cortex. Brain Res., *138:* 241-257.

Imig, T. J., and R. A. Reale 1977 The origins and targets of corticocortical connections related to tonotopic maps of cat auditory cortex. Neurosci. Abst., *3:* 8.

Imig, T. J., R. A. Reale and J. F. Brugge 1977 The origin and targets of primary field efferents related to tonotopic and binaural maps of cat auditory cortex. Proc. Int. Union Physiol., *12:* 706.

Jones, E. G., H. Burton and R. Porter 1975 Commissural and cortico-cortical "columns" in the somatic sensory cortex of primates. Science, *190:* 572-574.

Jones, E. G., and T. P. S. Powell 1968 The commissural connexions of the somatic sensory cortex in the cat. J. Anat., *103:* 433-455.

———— 1969 Connexions of the somatic sensory cortex of the rhesus monkey. II. Contralateral cortical connexions. Brain, *92:* 717-730.

Karol, E. A., and D. N. Pandya 1971 The distribution of the corpus callosum in the rhesus monkey. Brain, *94:* 471-486.

Knight, P. L. 1977 Representation of the cochlea within the anterior auditory field (AAF) of the cat. Brain Res., *130:* 447-467.

Merzenich, M. M., P. L. Knight and G. L. Roth 1975 Representation of cochlea within primary auditory cortex in the cat. J. Neurophysiol., *38:* 231-249.

Merzenich, M. M., and J. F. Brugge 1973 Representation of the cochlear partition on the superior temporal plane of the macaque monkey. Brain Res., *50:* 275-296.

Palmer, L. A., A. C. Rosenquist and R. J. Tusa 1978 The retinotopic organization of lateral suprasylvian visual areas in the cat. J. Comp. Neur., *177:* 237-256.

Pandya, D. N., M. Hallett and S. K. Mukherjee 1969 Intra- and interhemispheric connections of the neocortical auditory system in the rhesus monkey. Brain Res., *14:* 49-65.

Rose, J. E., N. B. Gross, C. D. Geisler and J. E. Hind 1966 Some neural mechanisms in the inferior colliculus of the cat which may be relevant to localization of a sound source. J. Neurophysiol., *29:* 288-314.

Shanks, M. F., A. J. Rockel and T. P. S. Powell 1975 The commissural fibre connections of the primary somatic sensory cortex. Brain Res., *98:* 166-171.

Shatz, C. 1977 Abnormal interhemispheric connections in the visual system of Boston Siamese cats: a physiological study. J. Comp. Neur., *171:* 229-246.

———— 1977b Anatomy of interhemispheric connections in the visual system of Boston Siamese and ordinary cats. J. Comp. Neur., *173:* 497-518.

Sovijärvi, A. R. A. 1973 Single-Neuron Responses to Complex and Moving Sounds in the Primary Auditory Cortex of the Cat. Academic Dissertation, Institute of Physiology, University of Helsinki, Helsinki, Finland.

Sovijärvi, A. R. A., and J. Hyvärinen 1974 Auditory cortical neurons in the cat sensitive to the direction of sound source movement. Brain Res., *73:* 455-471.

Suga, N. 1977 Amplitude spectrum representation in the Doppler-shifted-CF processing area of the auditory cortex of the Mustache bat. Science, *196:* 64-67.

Wilson, M. E. 1968 Cortico-cortical connections of the cat visual areas. J. Anat., *102:* 375-386.

Woolsey, C. N., and E. M. Walzl 1942 Topical projection of nerve fibers from local regions of the cochlea to the cerebral cortex of the cat. Johns Hopk. Med. J., *71:* 315-344.